ADVANCED MATERIALS

DOI: 10.1002/adma.200701790

Electric-Field-Assisted Growth of Highly Uniform and Oriented Gold Nanotriangles on Conducting Glass Substrates**

By *Panikkanvalappil R. Sajanlal* and *Thalappil Pradeep**

Size and shape control is a critical problem in the utility of nanomaterials as their physical and chemical properties depend strongly on structural parameters. Optical properties[1–3] and catalysis[4] of metal nanoparticles (NPs) reflect the structure-dependence most dramatically. Nanotriangles (NTs) or nanoprisms are a new class of nanomaterials and their properties such as near-infrared (NIR) absorption,[5–8] anisotropic electrical conductivity[9] and strong enhancement of electric fields at the vertices[10] are expected to make them useful for a variety of applications in photonics and optoelectronics, information storage, optical sensing,[11] biological labeling, imaging, metal enhanced fluorescence[12,13] and surface-enhanced Raman scattering (SERS).[14–16] Chemical,[17] photochemical,[18] and biological[10] routes for their synthesis in solution are documented. Precise control of size and shape of NTs is still a major unsolved issue and post synthetic procedures are necessary to obtain reasonable monodispersity. For many sensing and catalytic applications in nanotechnology, one requires a programmed assembly of such nanostructures on planar surfaces. Periodic arrays of triangles can be made by nanosphere lithography.[19] Several other strategies have been employed for the fabrication of NTs on planar surfaces such as seed mediation,[12,13] sputter deposition and thermal vapor deposition.[20] But ordered assembly is still a difficult task. In this report, we present an 'electrical potential assisted' method for the synthesis of uniform equilateral gold NTs, exhibiting preferred orientation having high near infrared absorption and strong surface enhanced Raman activity.

The method used here for the preparation of NTs is a combination of the seed mediated growth process[21] and the electrochemical deposition[22] of metal particles on conducting glass surfaces. The indium tin oxide (ITO) coated conducting glass surfaces were cleaned and nanoparticles were immobilized on them through a self assembled monolayer.[23] Afterwards, the potential assisted chemical growth was carried out as shown in the schematic (Fig. 1A) which resulted in highly uniform array of equilateral NTs on the ITO surface (see the Experimental Sec.).

The gold NTs formation on ITO substrate was studied by optical absorption measurements, atomic force microscopy (AFM) and dynamic force microscopy (DFM). Figure 1B shows the time dependent UV-vis-NIR spectra of the formation of NTs. Growth of seeds on the surface was confirmed from the characteristic absorption in the UV-vis spectrum, showing only one peak with a maximum at 529 nm (trace A, Fig. 1B). As the growth proceeds, there was the emergence of a broad peak in the NIR region. Also observed was a distinct color change of the nanoparticle coated ITO glass from colorless to magenta purple over a period 1 h. The peak in the NIR region is attributed to in-plane surface plasmon resonance (SPR) of NTs supported on ITO and that at 540 nm is due to their out of plane surface plasmon resonance.[10] The absorption centered in between 730–800 nm is attributed to the quadrupole resonance[17] of the nanotriangles. Weak intensity of this peak may be due to the surface contact of the NTs. Earlier reports[9,10] of NTs immobilized on substrates showed similar results. During the course of the NT growth, the intensity as well as the absorption maximum of the in-plane surface plasmon resonance increased. After a particular time interval, there was no apparent change observed in both the intensity as well as the absorption maximum which suggested that the NT growth stopped after 1 h. Even after 5 h of the growth process, there was no considerable change in the NIR absorption maximum compared to that after 1 h growth. Similar observations were also made by Mirkin et al.[24] for the solution phase growth of NTs. The red shift in the absorption maxima compared to the earlier reports of NTs[17] can be attributed to the increased edge length,[8,24] larger particle density,[25] increased surface contact[26] and extended delocalization of the in-plane electrons.[10] The slight red shift in the absorption maxima of the out of plane SPR is due to the smaller increase in the thickness of the NTs. A part of this intensity may also be due to spherical particles closer to the ITO surface, although not visible in AFM.

From the AFM analysis it was confirmed that all the triangles observed are equilateral (Fig. 2A) and have flat surfaces. Figure 2B is a 3D image of the nanotriangles formed after 1 h of growth, showing uniform and ordered stacking of the NTs.

[*] Prof. T. Pradeep, P. R. Sajanlal
DST Unit on Nanoscience
Department of Chemistry and Sophisticated Analytical Instrument Facility
Indian Institute of Technology Madras
Chennai – 600 036 (India)
E-mail: pradeep@iitm.ac.in

[**] We thank Department of Science and Technology, Government of India for constantly supporting our research program on nanomaterials. Thanks are due to Dr. T. Tsukuda, Institute of Molecular Science, Okazaki, Japan for allowing the use of his AFM facility for the DFM measurements. C. Subramaniam is thanked for assistance. Supporting Information is available online from Wiley InterScience or from the authors.

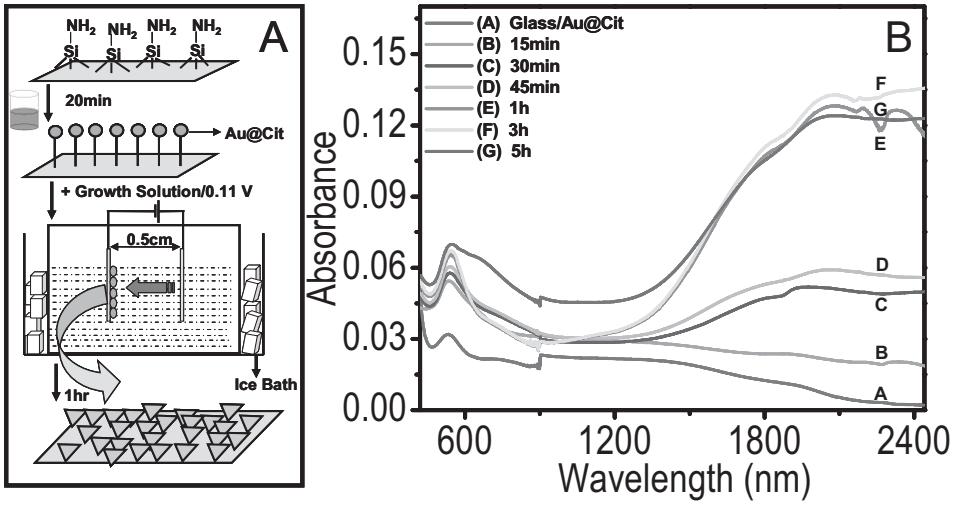

Figure 1. A) Schematic of the experimental process employed and B) UV-vis spectra of NT-coated ITO prepared using 10 mM Au^{3+} and by varying the time of growth.

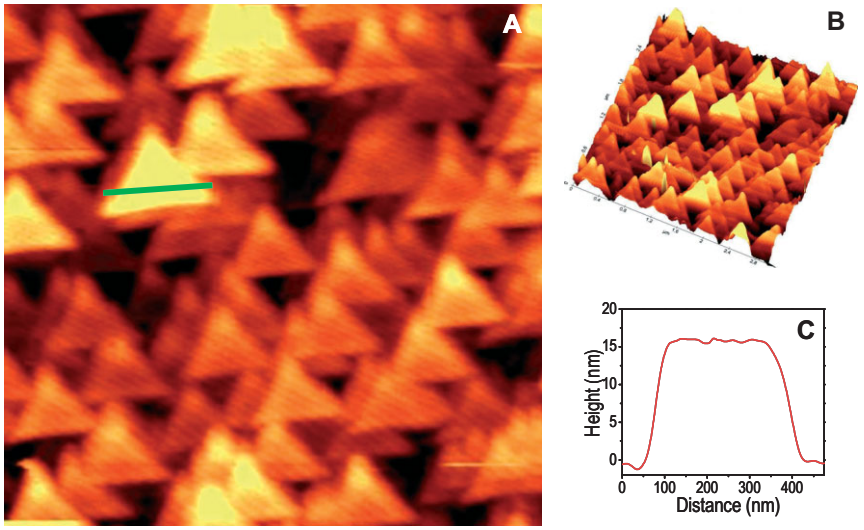

Figure 2. A) Contact mode AFM image (2 μm × 2 μm) of NTs formed on ITO after 1 h of growth B) Three dimensional (3D) view (3 μm × 3 μm) of the NTs and C) height profile of one NT along the dashed line in A. The NTs are found at different heights on the substrate and are stacked one over the other with a preferred orientation.

Edge lengths of NTs were measured from the height profile analysis (Fig. 2C). Out of twenty NTs analyzed, the average full width at half maximum (FWHM) of the NTs prepared after one hour growth was found to be (375 ± 15) nm with a thickness of (20 ± 5) nm. We note that all the triangles are arranged in a preferred direction. Although no spherical particles are visible in the surface topography, these could be present closer to the ITO plate. However, ultrasonication of the plates did not remove the particles or triangles.

We analyzed the NTs as well as the blank ITO by DFM (see Supporting Information 1). These images also revealed the formation of uniform and ordered NTs. In the X-ray diffraction (XRD) pattern of NTs, the (111) line is higher in intensity, suggesting that the NTs are lying flat on the surface, as seen in AFM. Note that the surface of NTs is composed of (111). The five diffraction peaks of face centered cubic (fcc) gold, (111), (200), (220), (311) and (222) are observed in the XRD (see Supporting Information 2).

We analyzed the sample after stopping the growth at various times. Figure 3A presents the contact mode AFM image of the NTs coated substrate after 30 min reaction. Uniform stacking of the NTs is confirmed from the 3D image. It was found that the upper surface of the NTs formed at this intermediate stage was not as flat as in Figure 2. The average edge length of the NTs was (200 ± 20) nm, shorter than the value found after complete growth. The average thickness was also smaller ((15 ± 5) nm). Even at this intermediate stage, we note that the orientation of the triangles is uniform.

In order to check the effect of the direction of the applied electrical potential, we did the experiment at the reverse potential. Figure S3 shows the AFM image of the ITO plate after 1 h of reaction by applying a potential of 0.11 V. A blank ITO plate was kept at the –ve terminal of the dc power supply and all other parameters were maintained constant. At this condition, the gold nanoparticles were grown largely to irregular structures. From this observation, it is clear that the direction of the applied potential also plays a major role in the NT formation.

The capability of ascorbic acid to reduce tetrachloroaurate to metallic gold in presence of metal particles is well

ADVANCED MATERIALS

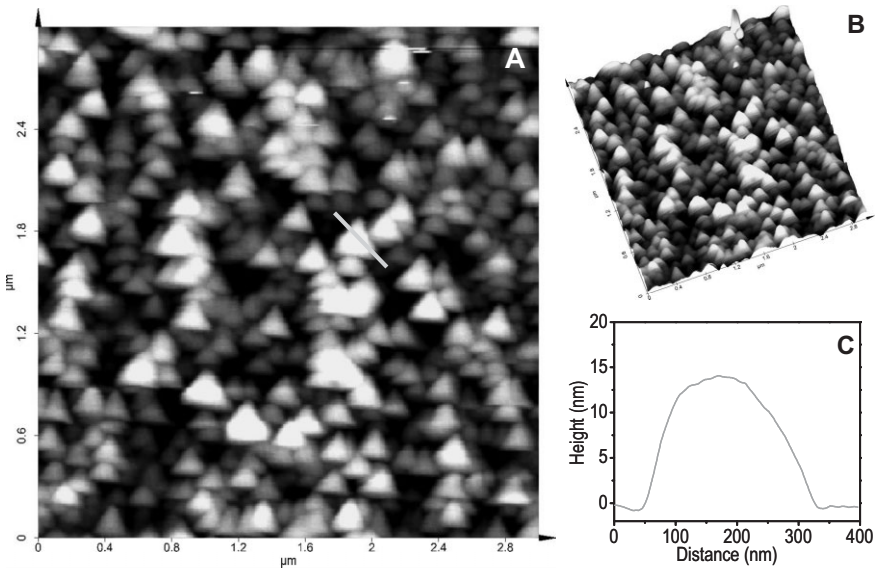

Figure 3. A) Contact mode AFM image (3 μm × 3 μm) of NTs formed on ITO after 30 min of growth. B) Three dimensional view (3 μm × 3 μm) of the NTs and C) height profile of one NT along the dashed line in A.

known.[27,28] In the present case, the electric field is inducing the growth of NPs to NTs in presence of the stabilizing agent, cetyltrimethylammoniumbromide (CTAB). Electric potential may enhance the preferential adsorption of CTAB to specific crystallographic planes. The reduction of Au ions occurs on the specific planes of Au seeds which are less stabilized by CTAB adsorption. This leads to the anisotropic growth of Au nuclei. The formation of NTs was not observed in the absence of the electric field confirming its critical role in the morphology determination. The growth is probably related to the enhancement of the electric field at the vertices of the NTs. We did a control experiment using blank ITO surface instead of the NP coated one, keeping all the other parameters constant. But no NTs were observed. It is reported[29] that lower temperature favors the formation of anisotropic NPs. The experiment has been conducted at room temperature instead of using an ice bath, which yielded poor growth. In the absence of electric field and at low temperatures, NPs nucleated nanorods.[30] This suggests that the electric field and temperature play major roles in the growth of NTs. The growth was studied on various ITO substrates with varying immersion times in the seed solution (to vary the surface coverage of the seed particles). Good yield was observed when we used an immersion time of 20 min.

In order to check the concentration dependence of Au^{3+} on the NT growth, we performed the reaction at increased concentration of Au^{3+} and ascorbic acid. However, poor monodispersity was observed under these conditions. Figure S4 shows the AFM image of the NTs formed when 1.4 mL of 10 mM Au^{3+} was used. The AFM image shows the presence of various shapes which included truncated triangles and some aggregated particles. We have monitored the NT formation at lower concentrations of gold and carried out the reaction using 500 μL of 10 mM Au^{3+}. In this case the perfect triangular shapes were not seen. The surfaces were not smooth (see Supporting Information 5). At the optimized condition, we used a growth solution which contains 20 mL of 0.1 M of CTAB, 900 μL of 10 mM Au^{3+} and 100 μL of ascorbic acid of 0.1 M to get perfect equilateral triangles in considerable yield. Figure S6 shows a large area AFM image of the NTs formed after 1 h of reaction at the optimized condition. This consists of perfect NTs. The potential applied and the distance between the electrodes were also optimized to 110 mV and 5 mm, respectively, to yield uniform NT growth. At higher potentials, we obtained irregular shapes. It may be noted that the synthesis of uniform NTs is strongly sensitive to the experimental parameters.

We investigated the possible enhancement of Raman active vibrational features of crystal violet (CV) molecules as a result of their adsorption on NTs. Distinct Raman features were observed even with 10 μL of 10^{-10} M CV on NTs (Fig. 4). The confinement of molecules in the hot spots[16] between the triangular nanostructures is the reason for the enhancement of their spectral characteristics.

In summary, we have demonstrated a novel methodology to fabricate highly aligned array of equilateral gold NTs on ITO substrates, which used a potential assisted seed mediated route. The NTs were characterized by AFM, DFM, XRD, and UV-vis-NIR spectroscopy. The film exhibited intense NIR

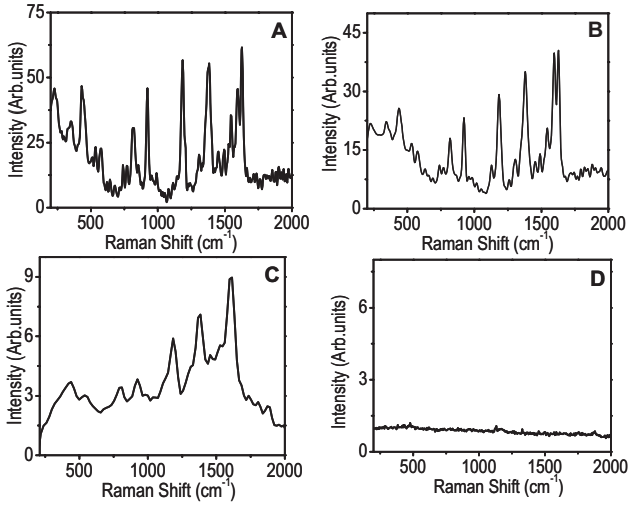

Figure 4. Raman spectra of A) pure solid CV on blank ITO, B) 10 μL of 5×10^{-8} M CV on NT coated ITO, C) 10 μL of 5×10^{-10} M CV on NT coated ITO, and D) 5×10^{-8} M CV on blank ITO.

absorption and strong surface enhanced Raman activity. These aligned arrays of NTs may have potential applications in optoelectronic devices, infrared filters and biosensors.

Experimental

Materials: Tetrachloroauric acid trihydrate ($HAuCl_4 \cdot 3H_2O$), CTAB, sodium citrate and ascorbic acid were purchased from CDH, India. Sodium borohydride ($NaBH_4$) and aminopropyltrimethoxysilane (APTMS) were purchased from Aldrich. One-side optically transparent conducting glass plates having an electrically conducting surface of ITO with a resistivity of 70 Ω cm^{-1} were used throughout this work. All chemicals were used as such without further purification. Triply distilled de-ionized water was used throughout the experiments.

Growth of Aligned Gold Nanotriangles on ITO Glass Surfaces: The following steps were used to prepare NTs on the substrate.

1. The ITO glass substrate (2 × 2 cm) was cleaned with a mild detergent solution, sonicated with deionized water and soaked in 10 % HCl solution for activation. They were then washed with water, dried and annealed at 450 °C for 7 h and cooled in a desiccator. The glass slides were dipped in 30 mM APTMS solution in methanol for 1 h. Afterwards, they were washed with methanol and water in sequence and kept at 110 °C for 2 h.

2. 4 to 8 nm diameter gold nanoparticle seeds were synthesized by taking 18.5 mL deionized water in a round bottom flask and 0.5 mL 0.01 M $HAuCl_4 \cdot 3H_2O$ and 0.5 mL 0.01 M aqueous trisodiumcitrate solution were added to it. Then 0.5 mL of ice cold 0.1 M aqueous $NaBH_4$ was added and stirred for 5 min.

3. The as prepared substrate was immersed in the seed solution (prepared in step 2) for a period of 20 min. The substrate was washed with water and dried.

4. Seed coated substrate and an identical blank ITO glass plate were kept at 5 mm apart such that the conducting surfaces faced each other and were connected to the –ve and +ve terminals of a DC power supply, as shown in schematic of Figure 1A. A Teflon spacer was used to maintain the distance. The growth vessel was kept inside an ice bath throughout the process. A potential of 110 mV was applied between the plates. The area of contact of both electrodes in the growth solution was fixed at 1 cm^2. 20 mL 0.1 M CTAB solution was added and kept for 3 min. After this, 900 μL 0.01 M $HAuCl_4 \cdot 3H_2O$ was added followed by 100 μL 0.1 M ascorbic acid. The set-up was allowed to stand undisturbed for 1 h. After the completion of growth, the substrate was taken out, washed using distilled water in order to remove the excess CTAB and was characterized using various spectroscopic and microscopic techniques. Experiments were also conducted after varying the parameters, as described in the text.

Instrumentation: Raman spectra and AFM were measured using AFM-CRM 200 spectrometer of WiTec GmbH. Contact mode AFM measurements were carried out using a reflux coated NANOSENSORS silicon cantilever. Sample was mounted on a piezo controlled scan stage. A diode laser of wavelength (980 ± 5) nm was used as beam deflector laser. The movement of the cantilever was detected using a segmented photodiode. For the vibrational characterization, the substrate was mounted on the sample stage of a confocal Raman microscope (CRM). The spectra were collected by the excitation of the sample with 514.5 nm Ar ion laser. The beam size used was <1 μm. The back-scattered light was collected by a 60X objective and sent to the spectrometer through a multimode fibre. The signals were then dispersed using a 1800 grooves/mm grating and the dispersed light was collected by a Peltier cooled charge coupled device (CCD). Data from liquid droplets were collected with a liquid immersion objective. UV-vis-NIR measurements were done using a Varian 5E spectrometer in the range of 200–2500 nm. A Seiko SPA-400 scanning probe microscope with silicon cantilever was used for the DFM measurements. XRD data were collected with a Shimadzu XD-D1 diffractometer using Cu Kα radiation (λ = 1.54 Å). The samples were scanned in the 2θ range of 10–90 degrees.

Received: July 22, 2007
Revised: September 19, 2007
Published online: February 12, 2008

[1] M. Maillard, S. Giorgio, M. P. Pileni, *Adv. Mater.* **2002**, *14*, 1084.
[2] I. Pastoriza Santos, L. M. Liz-Marzán, *Nano Lett.* **2002**, *2*, 903.
[3] A. P. Alivisatos, *Science* **1996**, *271*, 933.
[4] M. Chen, W. Goodman, *Acc. Chem. Res.* **2006**, *39*, 739.
[5] S. Porel, S. Singh, T. P. Radhakrishnan, *Chem. Commun.* **2005**, 2387.
[6] J. J. Diao, H. Chen, *J. Chem. Phys.* **2006**, *124*, 116103.
[7] S. S. Shankar, A. Rai, A. Ahmad, M. Sastry, *Chem. Mater.* **2005**, *17*, 566.
[8] D. C. Seong Ah, Y. J. Yun, H. J. Park, W. J. Kim, D. H. Ha, W. S. Yun, *Chem. Mater.* **2005**, *17*, 5558.
[9] A. Singh, M. Chaudhari, M. Sastry, *Nanotechnology* **2006**, *17*, 2399.
[10] S. S. Shankar, A. Rai, B. Ankamwar, A. Singh, A. Ahmad, M. Sastry, *Nat. Mater.* **2004**, *3*, 482.
[11] A. J. Haes, R. P. Van Duyne, *J. Am. Chem. Soc.* **2002**, *124*, 10596.
[12] K. Aslan, J. R. Lakowicz, C. D. Geddes, *J. Phys. Chem. B* **2005**, *109*, 6247.
[13] A. A. Umar, M. Oyama, *Cryst. Growth Des.* **2006**, *6*, 818.
[14] J. P. Schmidt, S. E. Cross, S. K. Buratto, *J. Chem. Phys.* **2004**, *121*, 10657.
[15] J. Zhang, X. Li, X. Sun, Y. Li, *J. Phys. Chem. B* **2005**, *109*, 12544.
[16] H. P. Lu, *J. Phys. Condens. Matter* **2005**, *17*, R333.
[17] J. E. Millstone, S. Park, K. L. Shuford, L. Qin, G. C. Schatz, C. A. Mirkin, *J. Am. Chem. Soc.* **2005**, *127*, 5312.
[18] R. Jin, Y. Cao, C. A. Mirkin, K. L. Kelly, G. C. Schatz, J. G. Zheng, *Science* **2001**, *294*, 1901.
[19] C. L. Haynes, R. P. Van Duyne, *Nano Lett.* **2003**, *3*, 939.
[20] D. Jia, A. Goonewardene, *Appl. Phys. Lett.* **2006**, *88*, 53105.
[21] B. Busbee, S. Obare, C. J. Murphy, *Adv. Mater.* **2003**, *15*, 414.
[22] C. D. Geddes, A. Parfenov, D. Roll, J. Fang, J. R. Lakowicz, *Langmuir* **2003**, *19*, 6236.
[23] C. Subramaniam, J. Chakrabarti, T. Pradeep, *Phys. Rev. Lett.* **2005**, *95*, 164501.
[24] J. E. Millstone, G. S. Métraux, C. A. Mirkin, *Adv. Funct. Mater.* **2006**, *16*, 1209.
[25] L. G. Olson, Y. S. Lo, T. P. Beebe, J. M. Harris, *Anal. Chem.* **2001**, *73*, 4268.
[26] M. D. Malinsky, K. L. Kelly, G. C. Schatz, R. P. Van Duyne, *J. Phys. Chem. B* **2001**, *105*, 2343.
[27] N. R. Jana, L. Gearheart, C. J. Murphy, *J. Phys. Chem. B* **2001**, *105*, 4065.
[28] J. Pérez-Juste, I. Pastoriza Santos, L. M. Liz-Marzán, P. Mulvaney, *Coord. Chem. Rev.* **2005**, *249*, 1870.
[29] A. Rai, A. Singh, A. Ahmad, M. Sastry, *Langmuir* **2006**, *22*, 736.
[30] Z. Wei, F. P. Zamborini, *Langmuir* **2004**, *20*, 11301.